

Dominant role of orbital splitting in determining cathode potential in $O3$ NaTMO_2 compounds

M. H. N. Assadi* and Y. Shigeta

Center for Computational Sciences, University of Tsukuba,
Tennodai 1-1-1, Tsukuba, Ibaraki 305-8577, Japan.

(Dated: 2018)

Designing high potential cathodes for Na-ion batteries, which are comparable in performance to Li-ion cathodes, remains a challenging task. Through comprehensive density functional calculations, we disentangle the relationship between the cathode potential and the ionicity of TM–O bonds in $O3$ NaTMO_2 compounds in which TM ions is a fourth- or fifth-row transition metal. We demonstrate that the magnetic exchange interaction and the local distortions in the coordination environment of TM ions play more significant roles in determining the cathode potential of the $\text{TM}^{3+} \rightarrow \text{TM}^{4+} + e^-$ reaction than the ionicity of the TM–O bonds in these compounds. These results indicate that designing cathode materials solely based on empirical electronegativity values to achieve high potential may not be a feasible strategy without taking into account a detailed structural assessment.

Keywords: Ionicity, Cathode potential, Na ion battery, *Ab initio*

INTRODUCTION

Layered transition metal (TM) oxides constitute an important materials category for cathode applications in rechargeable batteries. The fundamental operating principle for such cathodes is based on the availability of multiple oxidation states for the TM ion, which allows the removal or insertion of alkali metal atom from or into the framework of TM oxide while maintaining the materials integrity. Although Li atom is the most popular alkali metal atom in battery applications, the more affordable Na atom has been considered a suitable alternative for Li atom. Na atom, however, faces some challenges that need to be addressed before wide-scale industrial adaptation for portable applications becomes feasible [1]. For instance, Na atom has a larger ionic radius and smaller ionisation potential compared to those of Li atom resulting in lower performance [2, 3]. Consequently, to design competitive Na ion cathodes, all factors affecting the performance should be well understood and critically fine-tuned. One of such factors is the choice of TM that would possibly maximise the electrochemical potential of the cathode. It is generally speculated that the cathode potential is strongly correlated with the ionicity of the TM–O bond [3–5]. The more ionic the TM–O bond is, the stronger valence electrons are attracted by the TM nuclei. A stronger attraction, in turn, corresponds to higher energy for electron transfer, resulting in higher electrochemical potential upon the removal or the insertion of the alkali atoms [6]. In this communication, we examine this conjecture in detail to see if this correlation holds in layered sodium TM oxides of the $O3$ structure. Layered $O3$ structure, as shown in FIG. 1(a) is made of three alternating TMO_2 and Na layers arranged in hexagonal symmetry in which both TM and Na ions are octahedrally coordinated by oxygen. We chose this class of materials for our investigation because they are

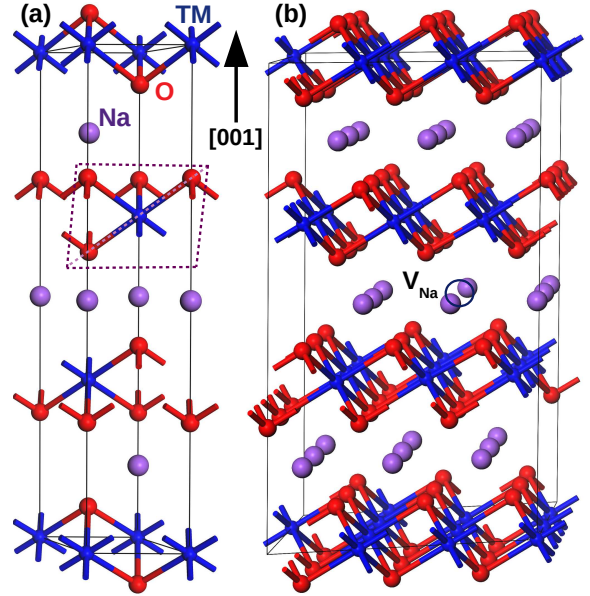


FIG. 1. The hexagonal representation of the $O3$ NaTMO_2 structure with $R\bar{3}m$ symmetry (space group 166) is presented in (a). Na, TM and O atoms occupy $3b$, $3a$ and $6c$ Wyckoff positions, respectively. The left panel (b) shows the $3a \times 3a \times 1c$ supercell used for calculating the sodium vacancy formation energy and cathode electrochemical potential.

among the most widely studied and commercialised Na ion cathode materials. We also considered all 3d and 4d TM ions for which +3 oxidation state is available.

METHODS

Spin-polarized density functional theory (DFT) calculations were carried out using augmented plane-wave method as implemented in VASP [7, 8]. The energy cut-off was set to 550 eV, while a k -point mesh was produced

by Monkhorst Pack scheme with a spacing of $\sim 0.02 \text{ \AA}^{-1}$ for Brillouin zone sampling. Hubbard term [9] (U_{eff}) was added to the 3d and 4d electrons to improve the accuracy of the electronic description through GGA + U approach. The U_{eff} values were 5 eV for 3d electrons and 2eV for 4d electrons, respectively. Lattice parameters and magnetic ordering of the TM ions of all compounds was fixed to the previously established ground state values [10]. A $3a \times 3a \times 1c$ supercell was used which is presented in FIG. 1(b) to calculate the formation energy (E_f) of the sodium vacancy (V_{Na}) and cathode potential. Using a relatively large supercell minimises the artificial vacancy-vacancy interaction that is caused by periodic boundary conditions [11].

RESULTS AND DISCUSSIONS

We used a single V_{Na} to simulate the early desodiation process. The cell voltage, V , is usually calculated using the following formula [12]:

$$V = \frac{-\{E_t(\text{Na}_y\text{TMO}_2) - E_t(\text{Na}_x\text{TMO}_2) - (y - x)E_t(\text{Na})\}}{(y - x)e}. \quad (1)$$

Here, E_t is the total energy of a given compound obtained by DFT calculations with the Hubbard U_{eff} correction. Na_yTMO_2 and Na_xTMO_2 are the sodiated initial and desodiated final compounds, respectively. On the other hand, E_f of creating one sodium vacancy in the supercell is given by the following standard equation [13]:

$$E_f = E_t(\text{Na}_n\text{TM}_n\text{O}_{2n}) - E_t(\text{Na}_{n-1}\text{TM}_n\text{O}_{2n}) - E_t(\text{Na}). \quad (2)$$

By comparing Eq. 1 with Eq. 2, we find that early in the desodiation process simulated by removing one Na atom from the supercell presented in FIG. 1, the following relationship holds: $V = -(E_f(V_{Na}))e$. This potential is presented in Table I. Along with the calculated values, the available experimental potentials for some of the compounds are also presented in Table I. The differences between the experimental and the calculated values are within the range of $\sim 0.5 \text{ V}$ which is satisfactorily accurate. By only considering the early desodiation process, that is removing only one Na atom from the supercell, we could avoid taking account of the complex and successive phase transitions during sodiation or desodiation processes. These phase transitions usually differ from compound to compound which can hinder a veracious theoretical assessment of the chemical trend [1]. Furthermore, the removal of one Na atom guarantees that in all supercells one TM^{3+} ion converts to TM^{4+} ion. This approach, therefore, offers us a straightforward insight into how the ionicity of the compound and the choice of TM ion affect the cathode potential while keeping all other possible variables constant. The ionicity of the TM-O bonds was determined by examining the electronic localisation function (ELF) [14]. ELF is defined as the

probability of finding a second like-spin electron near a given point. In the case of NaTMO_2 compounds, large ELF values ($1 - \sim 0.6$) peaking around the ionic centres is a characteristic of ionic bonding, while large ELF peaking in the area connecting two ions implies covalent bonding. The calculated ELF is plotted in FIG. 2 for all compounds, while the maximum ELF values (ELF_{Max}) for the given compounds are presented in Table I. The ELF was plotted along a plane containing an O-TM-O bond as marked by dashed lines in FIG. 1(a). No compound was found to have ELF_{Max} smaller than ~ 0.62 . Furthermore, ELF was larger around ionic centres, especially O, and decreased in the bond regions. These factors indicate that the TM-O in all studied compounds, with varying strength, were ionic.

ELF_{Max} values, presented in Table I, show that there is no clear trend relating the ionicity of the TM-O bonds in 3d TM containing NaTMO_2 compounds to the TM ions in the compound. For instance, NaTiO_2 , NaMnO_2 and NaNiO_2 are more ionic than their neighbouring compounds. However, the ionicity of 4d containing NaTMO_2 compounds monotonically increases as the atomic number of the TM ions increases. Additionally, there is no clear correlation between the cathode potential and the ionicity of the TM-O bonds either. The most obvious case is NaTiO_2 which has a negative potential value indicating the instability of Ti^{3+} ($t_{2g}^1 e_g^0$) and its preference for adopting Ti^{4+} ($t_{2g}^0 e_g^0$), though it has the most ionic TM-O bond among all compounds. Consequently, NaTiO_2 is indeed suitable for anode rather than for cathode application [15]. Furthermore, NaMnO_2 has a TM-O bond more ionic than both neighbouring NaCrO_2 and NaFeO_2 , but its potential is nonetheless smaller than the potentials of both those compounds. In this case, the creation of the V_{Na} transforms Mn^{3+} ($t_{2g}^3 e_g^1$) to Mn^{4+} ($t_{2g}^3 e_g^0$). Similarly, NaNiO_2 is also more ionic than the neighbouring- NaCoO_2 , although its potential is smaller than that of NaCoO_2 . In this case, upon the removal of one Na atom, a Ni^{3+} ($t_{2g}^6 e_g^1$) is transformed into Ni^{4+} ($t_{2g}^6 e_g^0$). For 4d TM containing compounds, the cathode potential did not follow the monotonic trend that governed the ionicity of the TM-O bonds with respect to the atomic number of the TM ions; NaTcO_2 and NaPdO_2 are both more ionic than the preceding NaMoO_2 , and NaRhO_2 respectively, but still have smaller cathode potential. The desodiation process transforms Tc^{3+} ($t_{2g}^3 e_g^1$) to Tc^{4+} ($t_{2g}^3 e_g^0$) in the first compound and Pd^{3+} ($t_{2g}^6 e_g^1$) to Pd^{4+} ($t_{2g}^6 e_g^0$) in the latter compound.

Based on the results obtained, we can so far conclude that when the desodiation brings a TM ion to an empty, half-filled or filled t_{2g} configurations ($t_{2g}^0 e_g^0$, $t_{2g}^3 e_g^0$, or $t_{2g}^6 e_g^0$) the cathode potential experiences a reduction compared to that of neighbouring TM ions in the same row. Furthermore, it also has become evident that the TM-O ionicity is not a good predictor of the cathode

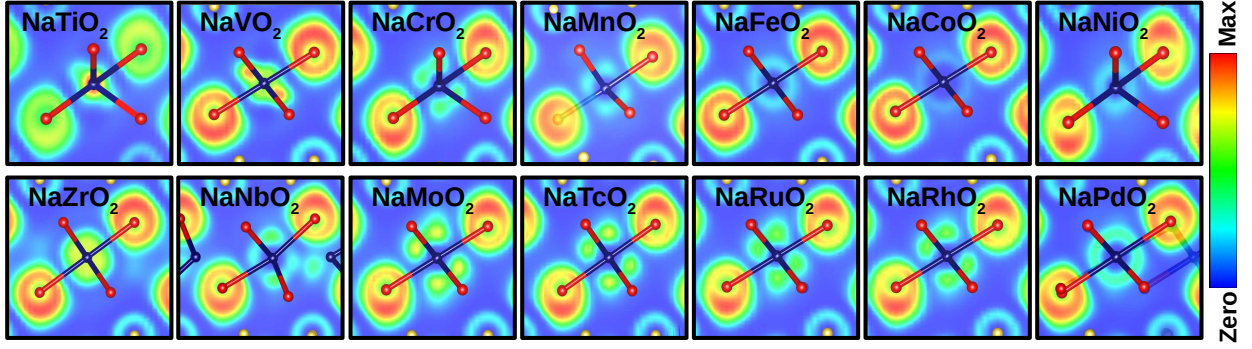


FIG. 2. The electronic localisation function plotted for planes containing O-TM-O bonds stretched from top right to left bottom of each panel. This plane is marked with dashed lines in FIG. 1(a). Red corresponds to the maximum ELF values presented in Table I while blue corresponds to zero ELF.

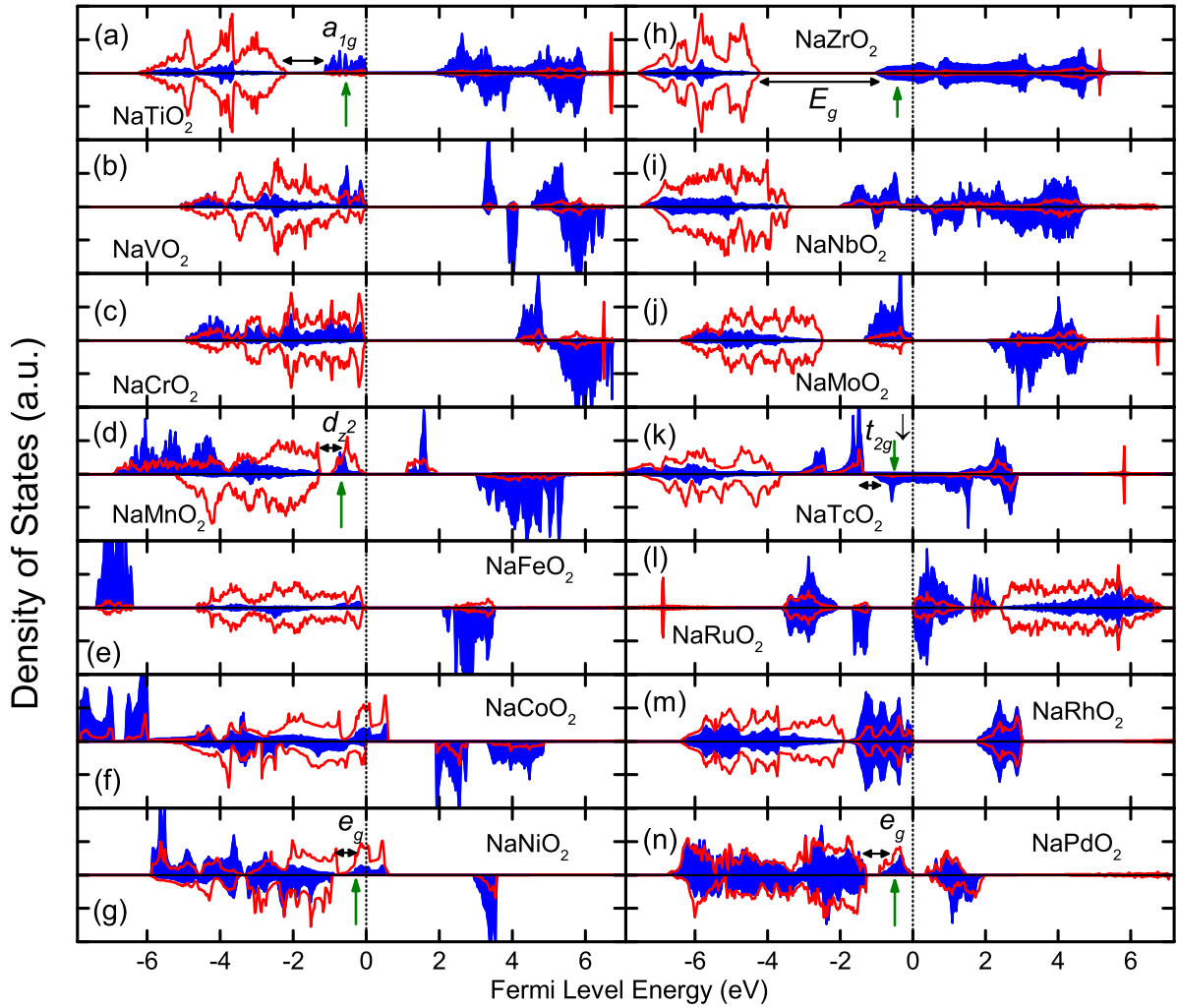


FIG. 3. The site projected density of states of a single TMO_2 chain in $O3$ NaTMO_2 compounds. The blue shaded areas correspond to the d states of a single TM^{3+} while the red lines correspond to the p states of the coordinating O ions.

potential. But why is it so? The redox in NaTMO_2 compounds is accomplished by the TM ions donating an electron upon the extraction of a Na atom. As a result, it is only the last valence electron with the highest energy level that determines the cathode potential. If such electron has a significantly higher energy level than the rest of the valence electrons, then the cathode potential will be relatively smaller even if the compound is overall highly ionic. This is because the ionicity of the TM–O bond is based on the overall electron affinity of the entire valence electrons to their respective ionic centres [16, 17].

Now, Lets examine what characteristics of the highest energy electron results in smaller potential. Examining the site projected density of states as presented in FIG. 3 reveals that when the last occupied TM^{3+} electron comes from a singly occupied orbital which is detached from the main valence band, the cathode potential is relatively smaller regardless of the ionicity of the TM–O bond. These detached orbitals are marked with green arrows for NaTiO_2 , NaMnO_2 , NaNiO_2 , NaTcO_2 and NaPdO_2 in FIG. 3. The detached orbitals can be created either by a magnetic exchange splitting in elements for which one spin channel is singly occupied or by a lattice distortion which splits the occupied states or simply in TM ions with single electron such as Ti^{3+} ion. The magnetic exchange splitting is a natural result of the spin-dependent Hamiltonian of the system. If the exchange splitting is larger than the spin channels bandwidth, and the spin minority channel is singly occupied, then the last occupied orbital becomes detached from the main valence band. This is the case in NaTcO_2 . In NaMnO_2 , a strong Jahn-Teller distortion [10, 18] favours high-spin configuration. However, the crystal field splitting of the spin-up e_g states is large enough that prevents the hybridisation of e_{z^2} orbital with the rest of the valence band. In NaNiO_2 and NaPdO_2 , the octahedral crystal field separates the fully occupied t_{2g} orbitals from the singly occupied e_g orbital.

In the compounds mentioned above, the detachment of the singly occupied orbitals is large enough that it creates a pseudo-gap within the valence band. As a result, the hybridisation between the highest energy TM electron and O 2p states which tend to gravitate towards the bottom of the valence band is significantly reduced. This lack of hybridisation further lowers the energy required for the redox reaction. This pseudo-gap is 1.112 eV in NaTiO_2 , 0.311 eV in NaMnO_2 , 0.422 eV in NaNiO_2 , 0.333 eV in NaTcO_2 and 0.374 eV in NaPdO_2 . In the case of NaZrO_2 in which a Zr^{3+} ($t_{2g}^1 e_g^0$) transforms to a Zr^{4+} ($t_{2g}^0 e_g^0$), the donated electron leaves the conduction band (also marked with a green arrow) instead of the valence band. In this case, the donated electron comes from orbitals higher in energy by the fundamental bandgap, i.e. 3.222 eV, than the bottom of the valence band.

As a final note, we would like to mention that according to Table I, the cathode potential is generally smaller

TABLE I. Maximum values for electronic localisation function (ELF_{Max}), the calculated cathode potential. When experimental data was available, the experimental cathode potential is also cited. The experimental potential corresponds to compounds that are nearly fully sodiated.

System	ELF_{Max}	Calculated Potential (V)	Experimental Potential (V)	Ref.
NaTiO_2	0.9360	−0.438		
NaVO_2	0.6446	2.127	~ 1.8	[19]
NaCrO_2	0.6843	3.610	~ 3	[20, 21]
NaMnO_2	0.6941	2.146	~ 2.5	[22]
NaFeO_2	0.6475	3.004	~ 3.4	[23, 24]
NaCoO_2	0.6426	4.129	~ 4	[25]
NaNiO_2	0.7120	1.987	~ 2	[26]
NaZrO_2	0.6524	−1.021		
NaNbO_2	0.6881	1.072		
NaMoO_2	0.6907	1.820	~ 1.1	[27]
NaTcO_2	0.6916	0.617		
NaRuO_2	0.7023	2.067		
NaRhO_2	0.7034	2.409		
NaPdO_2	0.7123	2.306		

for the 4d TM containing compounds than those for the 3d TM containing compounds. The smaller potential for 4d TM ions is typically expected as with increasing period; the more modest localisation effects lead to the weaker attraction between the electrons and the TM nuclei. Therefore, the use of 3d TM ions is preferred over the use of 4d TM ions for achieving high potentials.

CONCLUSIONS

In conclusion, we demonstrated when the extraction of a Na atom brings a TM ion to one of the $t_{2g}^0 e_g^0$, $t_{2g}^3 e_g^0$ or $t_{2g}^6 e_g^0$ configurations under octahedral coordination cathode potential is smaller than the case in which the final TM electronic configuration is otherwise. That is because of the last electron in TM^{3+} ion is detached from and less hybridised with the rest of the valence band orbitals. Expanding this concept to tetrahedral symmetry, we anticipate similarly that if compounds in which TM electronic configuration after desodiation was $e^0 t_2^0$, $e^2 t_2^0$, or $e^4 t_2^0$, the cathode potential would be potentially smaller. This electronic consideration has a stronger effect on determining the cathode potential than the ionicity of the TM–O bonds. At last, it is worth noting that our conclusions only hold if the redox reaction is fully compensated by the TM ion electrons and may not be readily generalised to compounds in which O ions also contribute to charge compensation during the redox reaction [28].

ACKNOWLEDGMENTS

This work was supported in part by MEXT as a social and scientific priority issue: Creation of new functional devices and high-performance materials to support next-generation industries to be tackled by using post-K Computer. Computational resources were provided by Kyushu University's high-performance computing centre and supercomputers at the Institute for Solid State Physics at the University of Tokyo and the Centre for Computational Sciences at the University of Tsukuba.

* h.assadi.2008@ieee.org

- [1] X. Xiang, K. Zhang, and J. Chen, *Adv. Mater.* **27**, 5343 (2015).
- [2] V. Palomares, P. Serras, I. Villaluenga, K. B. Hueso, J. Carretero-Gonzalez, and T. Rojo, *Energy Environ. Sci.* **5**, 5884 (2012).
- [3] C. Liu, Z. G. Neale, and G. Cao, *Materials Today* **19**, 109 (2016).
- [4] M. E. Arroyo-de Dompablo, M. Armand, J. M. Tarascon, and U. Amador, *Electrochem. Commun.* **8**, 1292 (2006).
- [5] P. Barpanda, G. Oyama, S.-i. Nishimura, S.-C. Chung, and A. Yamada, *Nat. Commun.* **5**, 4358 (2014).
- [6] B. C. Melot and J. M. Tarascon, *Acc. Chem. Res.* **46**, 1226 (2013).
- [7] G. Kresse and J. Furthmüller, *Comput. Mater. Sci.* **6**, 15 (1996).
- [8] G. Kresse and J. Furthmüller, *Phys. Rev. B* **54**, 11169 (1996).
- [9] S. Dudarev, G. Botton, S. Savrasov, C. Humphreys, and A. Sutton, *Phys. Rev. B* **57**, 1505 (1998).
- [10] M. H. N. Assadi and Y. Shigeta, *RSC Adv.* **8**, 13842 (2018).
- [11] M. J. Puska, S. Pykk, M. Pesola, and R. M. Nieminen, *Phys. Rev. B* **58**, 1318 (1998).
- [12] M. S. Islam and C. A. J. Fisher, *Chem. Soc. Rev.* **43**, 185 (2014).
- [13] C. G. V. d. Walle and J. Neugebauer, *J. Appl. Phys.* **95**, 3851 (2004).
- [14] A. D. Becke and K. E. Edgecombe, *J. Chem. Phys.* **92**, 5397 (1990).
- [15] D. Wu, X. Li, B. Xu, N. Twu, L. Liu, and G. Ceder, *Energy Environ. Sci.* **8**, 195 (2015).
- [16] D. Bergmann and J. Hinze, *Structure and Bonding* **66**, 145 (1987).
- [17] P. Politzer and J. S. Murray, *Theor. Chem. Acc.* **108**, 134 (2002).
- [18] T. Jia, G. Zhang, X. Zhang, Y. Guo, Z. Zeng, and H. Q. Lin, *J. Appl. Phys.* **109**, 07E102 (2011).
- [19] C. Didier, M. Guignard, C. Denage, O. Szajwaj, S. Ito, I. Saadoune, J. Darriet, and C. Delmas, *Electrochem. Solid-State Lett.* **14**, A75 (2011).
- [20] C.-Y. Yu, J.-S. Park, H.-G. Jung, K.-Y. Chung, D. Aurbach, Y.-K. Sun, and S.-T. Myung, *Energy Environ. Sci.* **8**, 2019 (2015).
- [21] X. Xia and J. R. Dahn, *Electrochem. Solid-State Lett.* **15**, A1 (2011).
- [22] X. Ma, H. Chen, and G. Ceder, *J. Electrochem. Soc.* **158**, A1307 (2011).
- [23] N. Yabuuchi, H. Yoshida, and S. Komaba, *Electrochemistry* **80**, 716 (2012).
- [24] J. Zhao, L. Zhao, N. Dimov, S. Okada, and T. Nishida, *J. Electrochem. Soc.* **160**, A3077 (2013).
- [25] T. Shibata, Y. Fukuzumi, W. Kobayashi, and Y. Moritomo, *Sci. Rep.* **5**, 9006 (2015).
- [26] P. Vassilaras, X. Ma, X. Li, and G. Ceder, *J. Electrochem. Soc.* **160**, A207 (2013).
- [27] L. Vitoux, M. Guignard, M. R. Suchomel, J. C. Pramudita, N. Sharma, and C. Delmas, *Chem. Mater.* **29**, 7243 (2017).
- [28] M. H. N. Assadi, M. Okubo, A. Yamada, and Y. Tateyama, *J. Mater. Chem. A* **6**, 3747 (2018).